OMAE'97

ICE RUBBLE BUILD-UP ON CONICAL STRUCTURES DURING RIDGE INTERACTIONS

R.F. McKenna and S.E. Bruneau
C-CORE, Memorial University of Newfoundland
St. John's, NF, CANADA, A1B 3X5

ABSTRACT

Ice tank experiments were conducted to address the interaction between fixed upward-breaking conical structures and first-year ice ridges. The present paper considers the accumulation of ice above the base of the cone and the resulting forces exerted on the structure. In total, fifteen experiments were conducted on six ice ridges with depths ranging from 0.6 m to 1.2 m. The experiments were unique because of the size of the ridges and the construction technique which resulted in realistic representations of first-year ridges. Horizontal and vertical loads were measured on the upward-breaking conical structure which had a neck diameter of 0.6 m, a slope of 45° and a base diameter of 1.8 m. Clearing forces on the cone were isolated by subtraction of the cyclical breaking forces for the refrozen layer. Since tests were conducted for different water levels, it was possible to assess the influence of the structure as well as ridge geometry on the rubble clearing forces. Comparisons were also made between the observed rubble build-up and calculations for limiting steady-state conditions.

INTRODUCTION

Conical and other sloping forms at the waterline are used to mitigate the large forces associated with ice crushing and to reduce ice-induced vibrations of offshore structures. The preferred designs for gravity base structures slope inward with increased elevation such that level ice is lifted on contact with the structure. In such cases, the vertical component of the load imparted to the structure partially offsets the moment applied by the horizontal load. As the slope of the structure is reduced with respect to the horizontal, level ice loads are reduced but the projected area exposed to ice rubble is increased. This is of considerable concern when such structures are impacted by large first-year ridges and rubble fields.

Ridge and rubble features are formed when ice is deformed in shear or compression. They are characterized by large accumulations of ice blocks, most of which are submerged. The above and below water portions of a ridge are termed sail and keel respectively as shown in Fig. 1. Following ridge formation, a refrozen layer of ice builds up at the waterline over the winter.

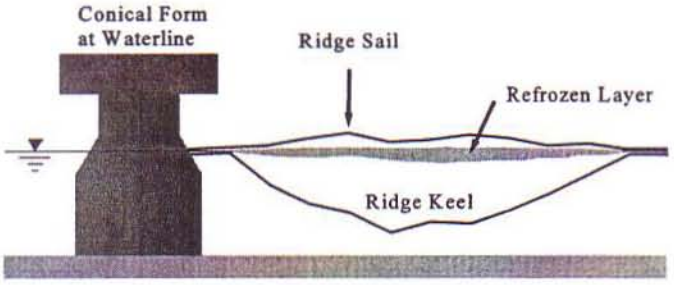

Fig. 1 Schematic of a first-year ice ridge impacting a conical structure

An upward-breaking conical structure will displace the sail rubble in its path, break the refrozen layer and may displace keel material as well. Because of the slope of the structure, a significant amount of rubble may accumulate on its front face. The loads exerted on the front face, exclusive of the cyclical loads for failure of the refrozen layer and global keel failure are termed the clearing loads.

Only a limited number of published experimental programs have addressed the interaction between first-year ice ridges and conical structures. Full-scale ice forces measured against an instrumented cone at the Kemi-I lighthouse have been documented by Määttänen and Mustamäki (1985), Hoikkanen (1985), Määttänen (1986) and Määttänen

and Hoikkanen (1990). While few details of the actual forces and rubble accumulations were reported, a maximum rubble height of 5 m was noted by Hoikkanen (1985). The forces and rubble accumulations due to ridges were not documented in the model tests reported by Määttänen and Mustamäki (1985). Timco and Cornett (1995) conducted scale model experiments with a conical bridge pier in ridges constructed of broken ice blocks. While realistic refrozen layers were simulated, the clearing forces on the conical portion of the structure were not isolated in these experiments.

The interaction between model ice ridges constructed from refrozen accumulations of broken rubble and faceted conical structures was investigated by Lau *et al.* (1993). The clearing forces for these experiments were analysed by Lau (1995), however the large floe sizes and strong refrozen layers were not representative of first-year conditions in temperate regions. For level ice moving against a faceted cone structure, Izumiyama *et al.* (1994) addressed the relation between the forces and the accumulated rubble. McKenna and Spencer (1994) also considered some of the mechanisms controlling clearing forces for level ice around a conical structure.

Experiments in first-year ridges were initiated at the Institute for Marine Dynamics in February 1995 with pilot experiments for a cylindrical structure (McKenna *et al.*, 1995a; McKenna *et al.*, 1997). These were followed by tests with a conical structure in June 1995 to address concerns regarding the design of the PEI bridge piers against large ridges (McKenna *et al.*, 1995b). Keel size, which was not varied in these experiments, was varied by a factor of 5 in a subsequent set of experiments (McKenna; 1996). Ice rubble clearing forces around the cone for this subsequent test series are the focus of the present paper.

The experiments are unique since the focus was on first-year ridges and the rubble shear strength was measured *in situ* (McKenna *et al.*, 1996; Bruneau *et al.*, 1996). The structure consisted of a cylindrical neck, a conical section about the waterline and a cylindrical base. The parameters which were varied in the experiments included the size and shape of the ridge, the speed of the interaction, the presence of a refrozen layer and the flexural strength of the rubble blocks. The height of the structure was varied to give a waterline diameter of between 1.2 m and 1.8 m. Added features of the present experiments include the isolation of the clearing component of the loads and the measurement of rubble accumulations against the cone.

EXPERIMENTAL SETUP

The tests were conducted in the ice tank at the Institute for Marine Dynamics in November and December, 1995. Six ice sheets were used in the test program and one or two ridges were constructed per ice sheet. All of the ridges were oriented at 90° to the direction of structure motion and stretched the entire 12 m breadth of the tank. For each ridge, two runs were made with the structure on parallel tracks 5.5 m apart. The ice sheets used for the present experiments have been labelled 4- 8 and 10 to correspond with the original reports.

The structure was mounted beneath the main test frame of the towing carriage. It consisted of a 45° upward-breaking conical ice shield and a separately instrumented cylinder as shown in Fig. 2. The base diameter of the cone was 1.83 m, its height was 0.613 m and it had a vertical neck 0.6 m high with a 0.605 m diameter. For the initial tests, the cylinder has diameter of 0.8 m and was 2.53 m long. For the last three ice sheets, a 1.80 m cylindrical collar, 1.6 m high, was fitted around the smaller cylinder.

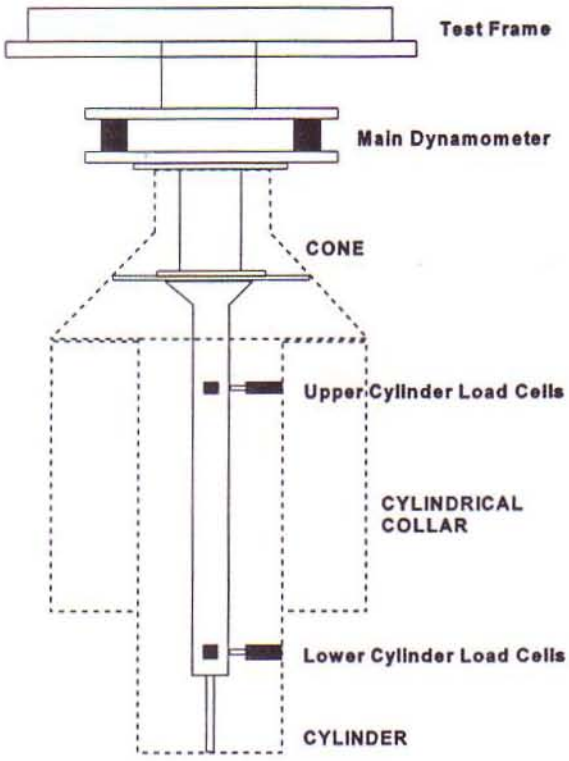

Fig. 2 Schematic of structure showing load measurement system

The cone and its supporting members were constructed of steel, while all of the cylinder components were constructed of aluminum. A plywood base was fitted to the exposed underside of the cone to prevent ice from accumulating inside. The base was removed to allow installation of the collar which was added to increase the cylinder diameter. During the tests with ice sheet 8, the collar slipped upward and rested against the cone, preventing the independent measurement of cylinder and cone loads.

The coefficient of sliding friction between the cone surface and ice blocks was measured to be 0.14 for a relative speed of 0.14 m/s (McKenna *et al.*, 1995b). These results were based on tests of blocks from the sail and from the level ice which were forces against a moving steel plate painted with the same coating as the cone.

ICE LOAD MEASUREMENT

Details of the load measuring system are illustrated in Fig. 3. A stiff structure spanning the test frame of the carriage was used to support the top plate of the main dynamometer. The dynamometer consisted of three six-axis load cells, a 100 kN cell mounted in front and two 50 kN cells mounted aft. Each cell was fixed to a ball joint to eliminate the transfer of moments. The base plate of the dynamometer supported a stiff column which was bolted to a horizontal plate welded to the inside of the cone. The central shaft of the cylinder was also connected to this plate and the outer shell of the cylinder was connected to this shaft via load cell arrangements at both top and bottom as shown in Fig. 3. For the cylinder, 12.5 kN capacity cantilever type load cells were mounted to

measure horizontal loads. At the top of the cylinder, a single cell measured Y (lateral) forces and two cells measured X (longitudinal) forces. At the base, the X and Y forces were measured using single cells.

In all, there were five axial forces measured in the cylinder and nine in the main dynamometer. These data were logged at 50 Hz after the signals were passed through 10 Hz anti-aliasing filters. Since the forces on the cylinder were measured independently, the forces on the cone were obtained by subtracting the cylinder loads from the total loads on the main dynamometer. For all of the tests except for the very slow ones, there was a 2 Hz oscillatory component to the force-time trace because of the rocking action of the cantilever structure. This was not exclusively a feature of the ice behaviour but also of the structure design. Because of this, all of the time traces were smoothed using a 1 Hz digital filter.

During the test program, the structure was run through open water in front of the ridge to isolate the hydrodynamic force. Since its effect was not more than a few Newtons, even for the 1.8 m diameter cylinder, it was ignored in the data processing.

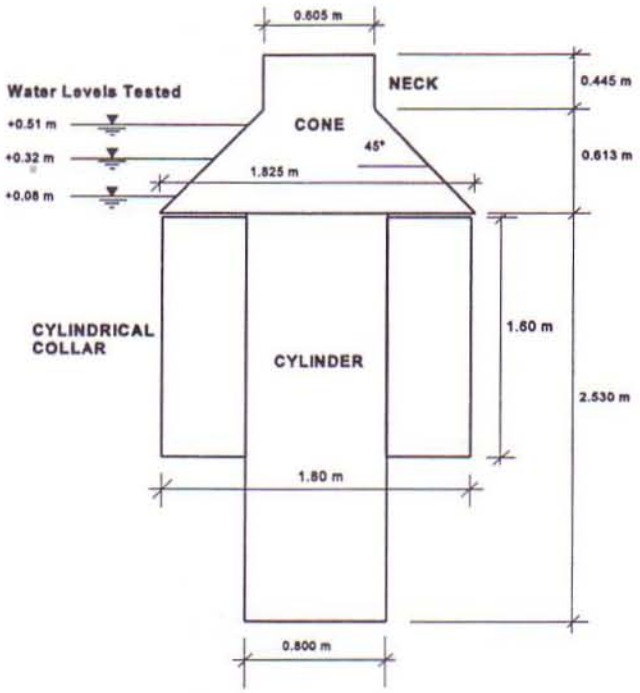

Fig. 3 Schematic of structure showing water levels tested

ICE CHARACTERISTICS AND RIDGE CONSTRUCTION

The ridges were constructed using a model ice with ethylene glycol as the primary additive. Fine bubbles were introduced into the ice during the freezing process to achieve a realistic density (Spencer and Timco, 1990). Each ridge was constructed by breaking level ice using the service carriage and placing the rubble between two saw cuts in the level ice. Two parallel ridges were constructed with ice sheets 7 and 8, and a single ridge was constructed for the other ones (Table 1). For all ice sheets except 6, the air temperature was reduced following ridge construction to form a thin refrozen layer. The freezing cycle was consistent for all ridges so it is expected that the properties of this layer were consistent from one ice sheet to the next. The thickness of the refrozen layer was measured manually and also using a thermistor probe with 1 cm resolution. While the refrozen layer thickness and strength were not test parameters, this 40 mm layer was included to provide the ridge keel with a realistic boundary condition at the top surface. Because the sail height varied across the ridge, the refrozen layer thickness was somewhat variable as well. Ice thickness data for the blocks in the ridge and for the refrozen layer are included in Table 1.

At the time of ridge construction, a number of ice blocks were submerged beneath the level ice sheet to simulate the thermal conditions present in the ridge keel. Ice blocks were also raised above the ice surface to simulate ridge sail conditions. Flexural strength was measured using a 3-point bending technique and the results are summarized in Table 1. The average flexural strength was 117 kPa for ice sheet 4 and 58 kPa for the other ones. The submerged blocks had an average strength of 31 kPa at test time for sheets 5 through 10, and an average of 82 for sheet 4. The sail blocks were considerably stronger at 170 kPa on average. The density of elevated and submerged blocks was measured at test time using an immersion technique and the results are reported in Table 2.

Due to the importance of the ridge profile on the applied forces, comprehensive measurements were made of the sail height and keel depth for all ridges. The total depth of the ridge at any one point was determined using a graduated aluminum rod pushed vertically through the ridge until no resistance was detected. The sail profiles were taken by measuring manually the distance from a fixed elevation on the service carriage to the ridge sail. The keel depth was taken as the difference between the total depth and the sail height measurements. Both sail and total depth measurements were made in duplicate at 0.5 m intervals across the width of the ridges.

Each ridge was profiled in four locations and summary data are given in Table 2. The length of level ice used to build a ridge and its thickness define the cross-section area of ice that went into the ridge which was used to estimate a rubble porosity. The average porosity calculated for all ice sheets was 0.22. Ice sheet 8 which was not included in the calculation since the estimated porosity was near zero, indicating most likely an error in the recorded length of level ice. This average porosity is less than the average value of 0.33 estimated for ridges of similar characteristics in McKenna *et al.* (1995b). These latter ridges were profiled using a 'chirp' acoustic system with transducers mounted to the moving video carriage which rolled on the bottom of the tank (McKenna *et al.*, 1997).

The difference between the two porosity estimates can be explained from the characteristics of the different measurement techniques. With the mechanical technique, the keel depth was determined at the point the rod met no further resistance. In contrast, the acoustic technique recorded the first returns and therefore the deepest points on the keel. Overall, the acoustic technique will always yield deeper keels and higher porosity estimates. An average of these two estimates gives a more representative value for porosity and this value of 0.26 has been used in the analysis of the clearing forces.

In situ measurements of the shear strength of the ridges were made using a vertical punch technique. As summarized in McKenna *et al.* (1996), a friction angle of 36° and an apparent cohesion of 0.44 kPa were estimated from data collected following ridge construction. The shear strength at test time was estimated to be 1.03 kPa. Similar results were obtained by Bruneau *et al.* (1996) for ridges constructed in the same manner using a direct shear technique.

TABLE 1 Ice thickness and flexural strength data

Ice Sheet	Ice Thickness: Level Ice at Time of Ridge Construction [mm]	Ice Thickness: Level Ice at Test Time [mm]	Ice Thickness: Consolidated Layer [mm]	Flexural Strength: Level Ice at Time of Ridge Construction [kPa]	Flexural Strength: Level Ice at Test Time [kPa]	Flexural Strength: Previously Submerged Blocks at Test Time [kPa]	Flexural Strength: Previously Elevated Blocks at Test Time [kPa]
4	46.8	57.9		138d 96u		112tt 51bt	
5	50.9	56.2		76d 43u	122d 76u	65tt 23bt	101tt 61bt
6	51.5	51.5		80d 43u	32d 18u	37tt 26bt	80tt 68bt
7	50.1	56.4		79d 40u	71d 88u 93tt 68bt	33tt 16bt	295tt 194bt
8	47.1	55.3		81d 52u	177d 156u	27tt 16bt	268tt 241bt
10	50.0	59.2	31 40#	52d 34u	132d 82u	30tt 27bt	270tt 195bt

Consolidated layer thickness from thermistor probe indicated by # - for cantilever tests, upward breaking strengths are suffixed u and downward are suffixed d - 3 point bending tests are tt for top in tension and bt for bottom in tension

TABLE 2 Ridge summary and test matrix

Ice Sheet	Run	Ridge Width [m]	Sail Block Density [kg/m^3]	Keel Block Density [kg/m^3]	Max. Sail Height [m]	Sail Area [m^2]	Keel Area [m^2]	Keel Area Above Base of Cone [m^2]	Water Level Relative to Base of Cone [m]	Test Speed [m/s]
4	1	3.5	787	903	0.13	0.30	2.44	1.23	0.32	0.070
4	2	3.5	787	903	0.13	0.30	2.44	0.29	0.08	0.070
5	1	4.0	746	895	0.24	0.53	2.83	0.34	0.08	0.070
5	2	4.0	746	895	0.24	0.53	2.83	0.34	0.08	0.070
6*	2	6.0	755	895	0.07	0.36	3.10	3.09	0.51	0.070
7	1	3.5	768	906	0.20	0.32	2.23	0.29	0.08	0.070
7	2	3.5	768	906	0.20	0.32	2.23	0.29	0.08	0.005
7	3	1.75	768	906	0.10	0.11	0.68	0.13	0.08	0.005
7	4	1.75	768	906	0.10	0.11	0.68	0.13	0.08	0.070
8	1	3.5	792	913	0.19	0.36	1.70	0.28	0.08	0.070
8	2	3.5	792	913	0.19	0.36	1.70	1.03	0.32	0.070
8	3	1.75	792	913	0.11	0.11	0.57	0.50	0.32	0.070
8	4	1.75	792	913	0.11	0.11	0.57	0.14	0.08	0.070
10	1	4.0	751	902	0.22	0.48	3.17	1.37	0.32	0.070
10	2	4.0	751	902	0.22	0.48	3.17	0.32	0.08	0.070

*All ridges had a refrozen layer except for ice sheet 6 which was tested shortly after ridge construction

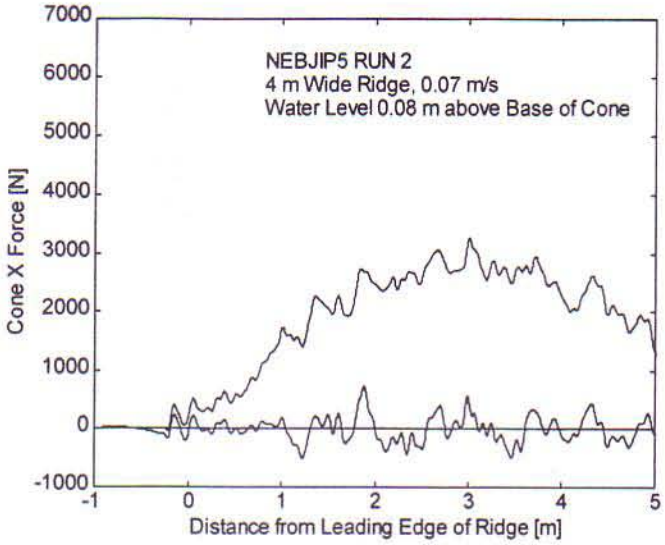

Fig. 4 Time series of cone forces for test 5 run 2 (lower line is same time series high-pass filtered to estimate breaking component)

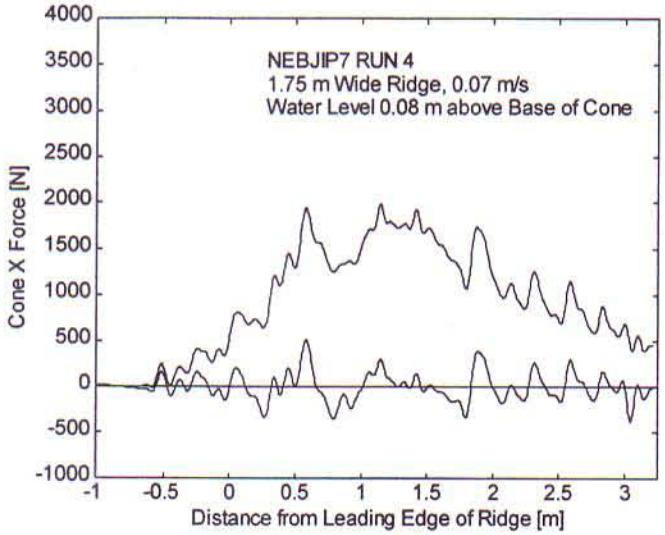

Fig. 5 Time series of cone forces for test 7 run 4 (lower line is same time series high-pass filtered to estimate breaking component)

TEST RESULTS

The experimental program consisted of 15 tests performed on 6 ridges as shown in the test matrix in Table 2. The ridge width, the presence of the refrozen layer, the structure speed and the elevation of the structure were varied in the tests. Except for sheet 6 where the ridge was wide and shallow, the ridges were approximately the same shape. This shape was ensured by scaling the ridge width by the square root of the length of level ice used to build the ridge. When a refrozen layer was present, most of the tests were performed with the waterline 0.08 m above the base of the cone and some were conducted with the water level 0.32 m above the base. For ridge 6 which did not have a refrozen layer, a water level of 0.51 m relative to the cone base was tested.

Samples of the load traces on the cone for ridge penetration are given in Fig. 4 and 5. Since the experiments were performed at constant speeds, the forces are plotted as a function of displacement which was calculated from the product of elapsed time and test speed. The displacements are for the front edge of the cone at the waterline and are referenced to the leading edge of the ridge. The peak forces on the cone and the penetration at peak force are summarized for all of the tests in Tables 3 and 4. Reference should be made to Table 2 which documents the corresponding test conditions.

TABLE 3 Forces on cone including interpreted clearing and breaking forces

Ice Sheet	Run	Mean X Breaking Force [N]	Mean Z Breaking Force [N]	Peak X Clearing Force [N]	Peak Z Clearing Force [N]	Peak X Total Force [N]	Peak Z Total Force [N]
4	1	964	770	4326	4310	5290	5080
4	2	1016	730	2764	1430	3780	2160
5	1	769	581	2421	2739	3190	3320
5	2	759	457	2531	1883	3290	2340
6	2	0	0	2600	2460	2600	2460
7	1	661	515	2179	1625	2840	2140
7	2	725	483	2505	1197	3230	1680
7	3	494	375	1416	1075	1910	1450
7	4	561	431	1449	1339	2010	1770
8	1	562	353	2248	2577	2810	2930
8	2	1227	694	4063	4086	5290*	4780
8	3	692	555	-	2585	-	3140
8	4	654	508	1356	1492	2010*	2000
10	1	1294	986	4736	5584	6030	6570
10	2	722	589	2388	2921	3110	3510

*estimated values based on test 4, run 1 and test 7, run 4 for similar conditions

CLEARING FORCES

The force-time traces on the conical portion of the structure shown in Fig. 4 and 5 contain a low frequency component. While rubble clearing and breaking of the refrozen layer may both contribute, the regularity of the cycles makes the latter more probable. It is assumed in the present analysis that the low frequency component is the force required to break the refrozen layer in flexure and it was isolated using the following procedure. The low frequency component of the traces was first removed using a high pass filter, allowing the distinct identification of peaks and troughs. For each run, the breaking component was then identified as the difference between the mean of the peaks and the mean of the troughs in the neighbourhood of the peak cone force. This quantity was then subtracted from the peak cone force to obtain a rubble clearing force. The analysis was performed for both the

TABLE 4		Cone penetration into the ridge at peak load		
Ice Sheet	Run	Ridge Width [m]	*Penetration at Peak X Force [m]	*Penetration at Peak Z Force [m]
4	1	3.5	2.2	2.2
4	2	3.5	2.4	2.5
5	1	4.0	4.1	4.1
5	2	4.0	3.0	4.3
6	2	6.0	4.8	5.3
7	1	3.5	1.9	3.1
7	2	3.5	2.0	4.1
7	3	1.75	0.9	2.1
7	4	1.75	1.1	1.3
8	1	3.5	1.5	2.3
8	2	3.5	-	2.0
8	3	1.75	-	1.3
8	4	1.75	-	1.8
10	1	4.0	3.0	3.0
10	2	4.0	1.8	3.1

* penetration distances are relative to the point where the leading edge of ridge met the front of the cone at the waterline

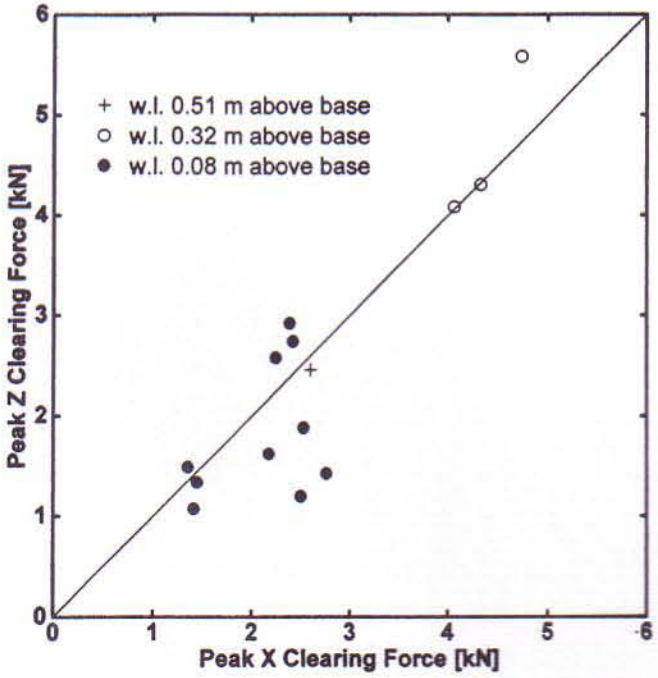

Fig. 6 Peak X clearing force as a function of peak Z clearing force (the line of equal X and Z forces is indicated)

X and Z cone forces and the data are listed in Table 3. The breaking component for test 8, runs 2 and 4 was obtained from the overall load on the structure.

The relation between peak X and Z clearing forces for all the tests is shown in Fig. 6. It appears that the force required to clear the rubble around the cone was approximately equal to the force required to lift it. For comparison, the ratio of vertical to horizontal forces to slide an ice block up a 45° slope is 0.75 when the coefficient of sliding friction is 0.14.

While the range of the test data is limited, it is of interest to establish scaling relations allowing the model data to be extrapolated to other scales. Level ice clearing forces on a conical structure are typically scaled by the ice thickness times the waterline diameter squared (hD_W^2) to represent a surcharge weight. Since the thickness of the rubble above the base of the cone is correlated with the waterline diameter, another scaling relation for the clearing forces is required for ridges.

An exhaustive regression study was carried out to identify the key test parameters associated with the clearing forces. Multiple linear regression coefficients were estimated for the raw data and for log-transformed data. In each case, the ridge width, the maximum sail height, the rubble cross-section area above the base and the waterline height had significant effects on the horizontal clearing forces. The test speed was not a significant parameter. The test plan was not designed to isolate the effect of all the test parameters and some of these were strongly correlated. Because of this, a regression on the logarithms of the parameters could not be derived from significant parameters while preserving the dimensionality of a proper scaling relation (i.e. a unit weight × m^3 or rubble shear strength × m^2).

If a physically-based scaling approach is to be developed, the weight of the rubble lifted by the structure is a likely candidate. Since neither the height of the rubble build-up nor the location of shear failure planes within the rubble is known *a priori*, the clearing forces were normalized by the weight of the rubble in the ridge contained within a vertical cylinder projected upward from the perimeter of the cone base. The geometry is illustrated in Fig. 7 in which D_B is the base diameter of the cone, D_W is the waterline diameter, H_W is the height of the waterline above the base of the cone and H_S is the sail height. The keel and sail rubble volumes around the front half of the 45° cone are then

$$V_K = \frac{\pi}{4}\left(D_B H_W^2 - \frac{2H_W^3}{3}\right) \qquad (1)$$

and

$$V_S = \frac{\pi}{4}\left[(D_B^2 - D_W^2)\frac{H_S}{2} + D_W H_S^2 - \frac{2H_S^3}{3}\right] \qquad (2)$$

Since most is the rubble is lifted onto the face of the cone, it is appropriate to use the actual rather than the buoyant weight of the keel rubble and the weight of the rubble contained in the projected cylinder is then

$$W_R = (1-p)g(\rho_{IK}V_K + \rho_{IS}V_S) \qquad (3)$$

where p is the porosity of the rubble, g is the acceleration due to gravity, and ρ_{IK} and ρ_{IS} are the densities of the ice in the keel and sail respectively. In Fig. 8, the horizontal peak clearing forces normalized with respect to W_R are plotted against, $(H_W+H_S)/H_N$, the ratio of rubble thickness to total height of the cone. The relations are shown for the peak and the average sail heights, and either could be used to fit the data. The least squares fit line relating the normalized clearing force F^* and normalized rubble thickness H^* is given. While the fits appear reasonable, there is a correlation between W_R and H_W+H_S which makes W_R suspect as a scaling factor.

Also shown in Fig. 8 are the clearing forces normalized by the area of the incoming rubble projected on the front of the cone, i.e. $D_B(H_W+H_S)-(H_W+H_S)^2$. In this case, the areas determined using the average and peak sail heights were multiplied by a rubble shear strength of 1 kPa to achieve a dimensionless force. The clearing forces normalized with respect to projected area did not have as significant a relation with height of rubble on the cone, indicating a better normalization. Neither the structure shape nor the ridge geometry were varied in the present tests so the present scaling relations can only be applied to a limited range of conditions.

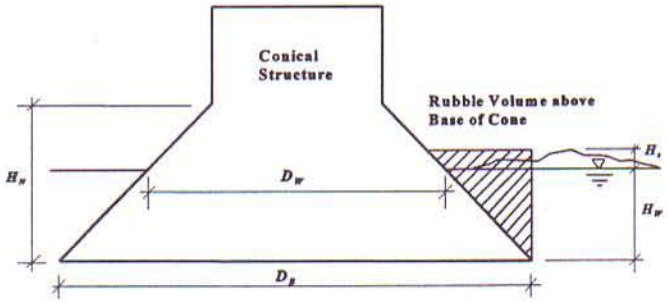

Fig. 7 Geometry used for rubble weight on cone in clearing force normalization

Fig. 9 View of rubble build-up around the structure during ridge interaction

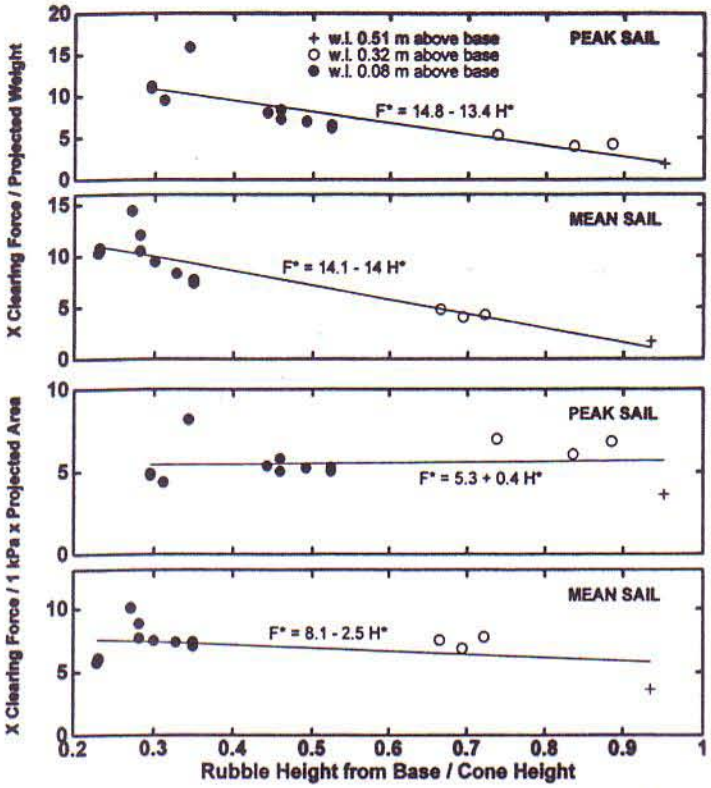

Fig. 8 Normalized X clearing force as a function of total rubble height / cone height

OBSERVATIONS OF ICE RUBBLE BUILD-UP

Video cameras were in operation at all times during the tests to record the rubble build-up. A fixed camera was placed 1 m above the water level and could be moved laterally to face the structure. The video image in Fig. 9 shows the structure advancing toward the camera. Another fixed camera was placed on one side of the structure, 2 m above the water level. When the structure was immediately adjacent to this camera, the view was obstructed and a hand-held camera was used instead.

A summary of the rubble measurements is given in Table 5. The measurements were made when the structure was half way through the ridge, which corresponds approximately to the penetration through the ridge at peak X force (Table 4). As the ridges were penetrated, the rubble heights tended to approach their maximum level soon after initial penetration and then remain constant with some variation through the interaction. The data in Table 5 have been identified as 'front' and 'side' to indicate accumulations on the front of the structure and clearing around the sides as shown in Fig. 10. The height of the rubble from the base of the cone and an average slope from the horizontal was measured in each case. The surcharge shape is indicated as straight when the slope was constant, humped when the slope at the top was shallower than below and curved when the convex surface had a slope which decreased with height. A rough shape was one which could not be categorized as above. For the 'side' data, the two values of the parameters correspond to those on each side of the structure. The maximum extent of rubble accumulation in front of the structure is also given for future reference.

TABLE 5 Maximum ice rubble build-up on cone measured from video

Ice Sheet	Run	Front				Sides		
		Max. Height from Base [m]	Extent from Neck [m]	Surcharge Slope [°]	Surcharge Shape	Max. Height from Base [m]	Surcharge Slope [°]	Surcharge Shape
4	1	1.10	0.95	-	curved	-	-	-
4	2	0.85	-	-	-	0.85(North) 0.80(South)	29 33	straight straight
5	1	0.85	0.90	30	straight	0.70 0.70	29 29	hump rough
5	2	0.85	-	-	-	0.75 0.70	35 22	curved curved
6	2	-	-	-	-	-	-	-
7	1	0.85	0.80	35	hump	0.75 0.75	34 34	hump straight
7	2	0.85	-	-	-	0.85 0.75	39 30	straight straight
7	3	0.80	-	-	-	0.75 0.70	32 40	-
7	4	0.80	0.85	33	straight	0.65 0.70	36 39	-
8	1	0.85	0.90	33	hump	0.75 0.80	39 45-20	straight hump
8	2	-	-	-	-	-	-	-
8	3	-	-	-	-	-	-	-
8	4	0.80	0.85	36	straight	0.70 0.75	30 35	straight straight
10	1	1.10	1.00	29	straight	0.85 1.05	26 28	rough rough
10	2	0.85	-	-	-	0.90 0.80	33 33	straight straight

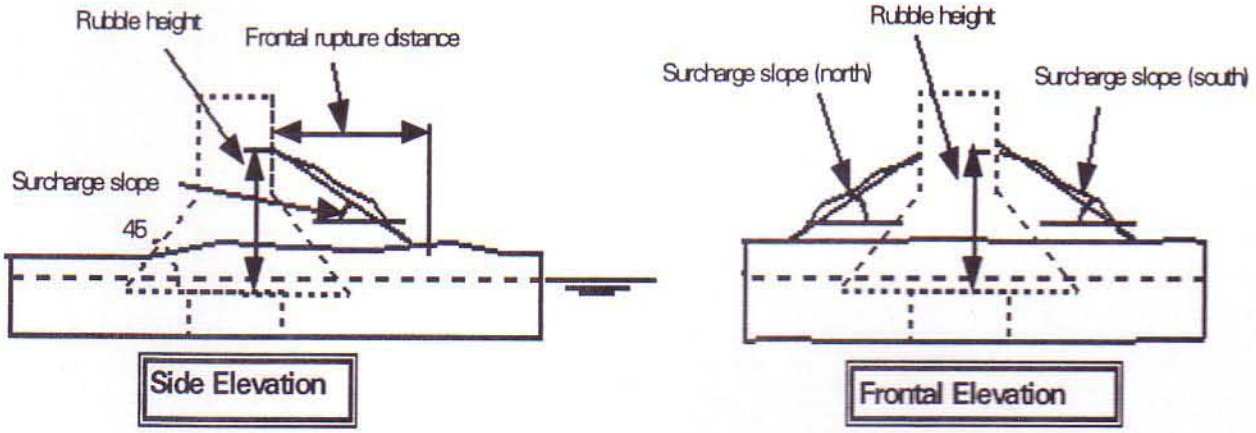

Fig. 10 Measurement details for rubble accumulations

In all cases, the rubble rose above the height of the neck (0.61 m from the base) both on the sides and on the front. Similar accumulations were observed on the front and sides, although the ice rose higher on average at the front. The highest measurements were recorded for test 4, run 1 and test 10, run 1 when the waterline was 0.32 m above the base of the cone. Other runs at this height may also have had high rubble accumulations but measurements could not be made because the video camera was obstructed.

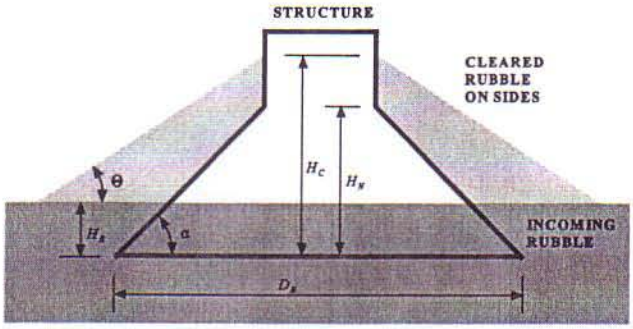

Fig. 11 Schematic showing parameters in steady-state model for rubble build-up

ESTIMATES OF RUBBLE BUILD-UP FOR STEADY STATE CONDITIONS

As a first-year ridge moves past a conical structure, rubble builds up slowly on the cone and is shed when the ridge has passed. For a very wide ridge, the ice tends to reach a stable height which is maintained for some distance. In this case, the rubble passing the sides of the cone must be the same as that displaced by the structure. A simple model was outlined previously by McKenna and Spencer (1994) encompassing this idea. In the present situation, it was implemented by assuming that the rubble moved past the cone at the same speed as the ridge advance and that its density was not altered in the process.

Consider the incoming rubble with height H_R above the base of the cone as shown in Fig. 11. This is displaced to the sides of the structure, forming an angle θ with the horizontal and rising to a height H_C. As long as the speed of the rubble passing the sides is the same as the incoming rubble, the area of the rubble cleared on the sides is equal to the projected area of the incoming rubble onto the cone, i.e.

$$H_R\left(D_B - \frac{H_R}{\tan\alpha}\right) = \frac{(H_C - H_R)^2}{\tan\theta} - \frac{(H_N - H_R)^2}{\tan\alpha} \qquad (4)$$

where α is the cone slope from the horizontal, D_B is the base diameter of the cone and H_N is the height of the neck above the base of the cone. From this relation, the height of the cleared rubble can be expressed as

$$H_C = H_R + \left\{\left[H_R\left(D_B - \frac{H_R}{\tan\alpha}\right) + \frac{(H_N - H_R)^2}{\tan\alpha}\right]\tan\theta\right\}^{1/2} \qquad (5)$$

A similar relation can be obtained when the height of rubble is less than the neck height. The relation between H_C and θ defined by Eq. (5) is plotted in Fig. 12 for the present cone angle of α=45°and neck height of H_N=0.61 m. It is expected that the level of the incoming ice should be at least the average sail height (ridge cross-section area above cone base / ridge width from Table 2) and not more than the peak sail height. The rubble height H_R was estimated for each of these cases by calculating average values for the larger ridges (W = 3.5 m and 4.0 m) based on the data in Table 2. Lines for waterline levels of 0.08 m and 0.32 m above the cone base are plotted.

The data from Table 5 for the sides of the cone are also shown in Fig. 12. Each data point was obtained by averaging the values for the two sides of the cone. Based on Fig. 12, Eq. (5) provided reasonable estimates for the rubble accumulation at the sides of the cone for average sail heights. Using peak sail height, this equation also provided a reasonable upper bound for the data. The data in Table 5 indicate that rubble heights at the front and sides of the cone are closely related. Eq. (5) may therefore be used to estimate rubble heights around the front face of conical structures impacted by first-year ridges.

Since the present data are for a narrow range of conditions, some caution should be exercised when applying Eq. (5) to other ridge and structure geometries. For example, very steep structures would not tend to lift as much rubble onto the conical face. As well, it should be noted that the refrozen layer in the present experiments was thin and was not a significant factor in the rubble accumulations.

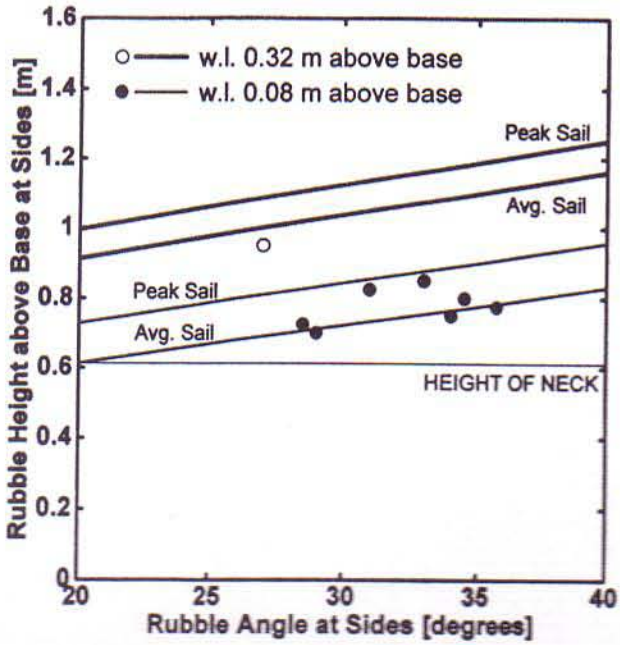

Fig. 12 Comparison of observed rubble accumulations (symbols) and estimated heights (lines) from Eq. (5)

CONCLUSIONS

Fifteen scale model tests were performed on six ridges to address the forces and mechanisms of first-year ridge failure against a 45° upward-breaking conical structure. The experiments are unique since they address the behaviour of first-year ridges modelled in a realistic manner and at a large scale. Extensive measurements were made of the properties of the blocks forming the ridge and of the shear strength of the rubble *in situ*. The parameters addressed in the test program were ridge size, water level and structure speed.

The clearing forces on the conical portion of the structure were found to depend on ridge size and water level, and scaling relations were obtained to describe them. Observations were made of the rubble build-up around the structure and these can be predicted using a steady-state model of the process.

ACKNOWLEDGEMENTS

The experiments were funded by PERD/NEB under project 6A5014 *Ice forces on Conical Structures* and by K.R. Croasdale and Associates on behalf of the Rubble JIP partners: Exxon Production Research Company and Mobil Research and Development Corporation. Ken Croasdale, Chris Heuer (Exxon) and Walt Spring (Mobil) assisted with the development of the test plan. C-CORE completed the work under contract to the Institute for Marine Dynamics. Stephen Jones administered the project on behalf of the Institute for Marine Dynamics. Ice tank personnel Brian Hill and Craig Kirby assisted with all aspects of the experiments, and Mary Williams assisted with the rubble properties experiments.

REFERENCES

Bruneau, S.E., McKenna, R.F., Croasdale, K.R., Crocker, G.B. and King, A.D. (1996) *In situ* direct shear of ice rubble in first-year ridge keels, in Proceedings of the 49th Canadian Geotechnical Conference, St. John's, Newfoundland, Vol.1, pp.269-278.

Hoikkanen, J. (1985) Measurement and analysis of ice forces against a conical offshore structure, in Proceedings of the 8th International Conference on Port and Ocean Engineering under Arctic Conditions (POAC), Narssarssuaq, Greenland, Vol. 3, pp.1203-1220.

Lau, M., Jones, S.J., Tucker, J.R. and Muggeridge, D.B. (1993) Model ice forces on a multi-faceted cone, in Proceedings of the 12th International Conference on Port and Ocean Engineering under Arctic Conditions (POAC), Hamburg, Vol. 2, pp.537-546.

Izumiyama, K., Irani, M.B. and Timco, G.W. (1994) Influence of a rubble field in front of a conical structure, in Proceedings of the Fourth International Offshore and Polar Engineering Conference (ISOPE), Osaka, Japan, Vol.2, pp.553-558.

Lau, M. (1995) Piece size and component force analysis of data collected during a multi-faceted cone experiment, report prepared for the Institute for Marine Dynamics, IMD report CR-1995-03.

Määttänen, M. (1986) Test cone project, in Proceedings of PolarTech '86, Espoo, Finland, Vol. II, pp.749-761.

Määttänen, M. and Hoikkanen, J. (1990) The effect of ice pile-up on the ice force of a conical structure, in Proceedings of the 10th IAHR Ice Symposium, Espoo, Finland, pp.1010-1021.

Määttänen, M. and Mustamäki, E.O. (1985) Ice forces exerted on a conical structure in the Gulf of Bothnia, in Proceedings of the 11th Annual Offshore Technology Conference (OTC), Houston, pp.313-320.

McKenna, R.F. (1996) First-year ice ridge forces on upward breaking conical structures, contract report prepared for Institute for Marine Dynamics, National Research Council of Canada, C-CORE Publication Number 96-C11.

McKenna, R.F., Bruneau, S.E. and Guzzwell, J.A. (1997) Modelling unconsolidated rubble forces on a cylindrical structure, this volume.

McKenna, R.F., Bruneau, S.E. and Williams, F.M. (1996) *In situ* shear strength measurements of model ice rubble using a punch technique, in Proceedings of the 49th Canadian Geotechnical Conference, St. John's, Newfoundland, Vol.1, pp.279-286.

McKenna, R.F., Bruneau, S.E., Guzzwell, J.A., Hill, B. and Kirby, C.S. (1995a) Pilot experiments with a cylindrical structure in unconsolidated ridges, Contract report prepared for the National Energy Board, NRC/IMD Report TR-1995-20.

McKenna, R.F., Williams, F.M. Hill, B. and Kirby, C.S. (1995b) Forces on the Northumberland Strait bridge piers due to ice ridge keels, Contract report prepared for Public Works and Government Services Canada, NRC/IMD Report TR-1995-38.

McKenna, R.F. and Spencer, D. (1994) Ice rubble buildup on conical structures, in Proceedings of the 12th International Symposium on Ice, International Association for Hydraulic Research (IAHR) Vol. 1, pp.177-186.

Spencer, D. and Timco, G.W. (1990) CD model ice: a process to produce correct density (CD) model ice, in Proceedings of the 10th IAHR International Symposium on Ice, Espoo, Finland, Vol. 2, pp.745-755.

Timco, G.W. and Cornett, A.M. (1995) Model tests of ridge interaction with a bridge pier for the Northumberland Strait crossing, Contract report prepared for Public Works and Government Services Canada, NRC/IMD Report TR-1995-02.